Research Article Vol. 7, No. 8 / August 2020 / Optica 995

optica

In situ temporal measurement of ultrashort laser pulses at full power during high-intensity laser–matter interactions

HELDER M. CRESPO,[1,*] TOBIAS WITTING,[2,4] MIGUEL CANHOTA,[1] MIGUEL MIRANDA,[1,3] AND JOHN W. G. TISCH[4]

[1]IFIMUP and Departamento de Física e Astronomia, Faculdade de Ciências, Universidade do Porto, R. do Campo Alegre s/n, 4169-007 Porto, Portugal
[2]Present Address: Max Born Institute for Nonlinear Optics and Short Pulse Spectroscopy, Max-Born-Straße 2 A, 12489 Berlin, Germany
[3]Sphere Ultrafast Photonics, R. do Campo Alegre 1021, Ed. FC6, 4169-007 Porto, Portugal
[4]Blackett Laboratory, Imperial College, London SW7 2AZ, UK
*Corresponding author: hcrespo@fc.up.pt

Received 21 May 2020; revised 10 July 2020; accepted 14 July 2020 (Doc. ID 398319); published 11 August 2020

In laser–matter interaction experiments, it is of paramount importance to characterize the laser pulse on target (*in situ*) and at full power. This allows pulse optimization and meaningful comparison with theory, and it can shed fundamental new light on pulse distortions occurring in or on the target. Here we introduce and demonstrate a new technique based on dispersion-scan using the concurrent third harmonic emission from the target that permits the full (amplitude and phase), *in situ*, in-parallel characterization of ultrashort laser pulses in a gas or solid target over a very wide intensity range encompassing the 10^{13}–10^{15} Wcm^{-2} regime of high harmonic generation and other important strong-field phenomena, with possible extension to relativistic intensities presently inaccessible to other diagnostics.

https://doi.org/10.1364/OPTICA.398319

1. INTRODUCTION

Great progress has been made over the last 20 years in the development of techniques such as FROG [1], SPIDER [2], MIIPS [3], and more recently, dispersion-scan (d-scan) [4], to fully characterize femtosecond laser pulses, that is, to measure the amplitude and phase of the optical field. This capability has been vital for the development of few-cycle lasers [5–7] whose pulses contain just a small number of optical cycles or even a single cycle [8]. Knowledge of the pulse phase allows for the dispersion to be precisely controlled to achieve the shortest pulses possible—often very close to the transform limit. A full characterization is also critical to properly optimize and interpret experiments where ultrashort pulses are used to trigger and probe dynamics in quantum systems. Such experiments include high harmonic generation (HHG), e.g., for attosecond pulse generation [9,10] and for accessing the electronic structure of solids [11], and laser-plasma particle acceleration [12–14].

However, existing pulse characterization techniques have limitations. They usually require complex setups, especially for the measurement of few-cycle pulses that are extremely sensitive to small amounts of dispersion that they accumulate as they propagate through optics and even air. For example, a 4 fs pulse with a spectrum centered at a wavelength of 800 nm is broadened to ≈25 fs by passing through 1 mm of fused silica or 1.6 m of air. Hence, great care must be taken to ensure that the pulse measurement is representative of the pulse at the desired location. For many experiments, including those that involve HHG and laser-plasma generation in gases, this location is within a gas target inside a vacuum chamber into which the laser pulse is focused to very high intensity. This poses two challenges. The first is that this is often many meters from the measurement device. The usual practice is to try and ensure equal material dispersion in the beam paths to the measurement device and to the gas target, or to account for any differences numerically. This is subject to error that can be significant for very short pulses. The second challenge is that the standard benchtop diagnostics are unable to measure pulses at the high intensities used in the experiment due to saturation and damage effects. Hence, a much lower intensity pulse reflection is sent to the diagnostic. Such a measurement therefore does not account for a nonlinear phase accumulated by the higher intensity pulse travelling to the experiment, and within the experiment itself.

The ability to fully characterize ultrashort laser pulses *in situ* (i.e., within the target) at high intensity enables pulse optimization and the quantification of time-dependent dynamics within the same experiment. This is very important for testing and validating new models, and for coherent control of strong-field processes, but it has proven very difficult to achieve. A complete on-target pulse characterization can be performed with attosecond streaking

[15,16] or attosecond transient absorption [17]. However, these methods must be carried out at lower intensity in a second, usually lower density target, not the gas target used for HHG. They are also complex due to the requirement of attosecond pulse generation and electron- or XUV-spectroscopy.

The ARIES technique [18] and the petahertz optical oscilloscope [19] are all-optical schemes capable of measuring a weak time-dependent optical field in a HHG gas target by measuring its perturbing effect on a much stronger field. They require a second ultrafast laser pulse that can be precisely delayed with the pulse to be measured, and the measurement information is mapped onto the high harmonics, and hence a series of specific XUV spectroscopic measurements is needed for the pulse retrieval. The TIPTOE technique [20] has a simple electrical current readout, but it is similar in that a weak pulse is measured through its perturbing effect, in this case on tunnel ionization in a gas target driven by a stronger field. Although they require elaborate setups, the aforementioned techniques are able to retrieve the full time-dependent optical field, and thus they resolve the pulse carrier envelope phase (CEP), which is not usually accessible with standard benchtop diagnostics, such as SPIDER, FROG, or d-scan.

An *in situ* technique based on SPIDER that retrieves the field up to an uncertainty in the CEP has been used to measure weak (150 nJ) 5 fs pulses in a gas ionized by a long pump pulse [21], but the required low intensities seem to preclude accessing the strong-field regime. STARFISH [22] is an all-fiber interferometric technique that directly measures the spatiotemporal and spatio-spectral structure of few-cycle pulses at any given plane along the propagation direction (including at a focus) [23], but it requires scanning a fiber tip in two dimensions within that plane. Spatially resolved Fourier transform spectrometry [24] and TERMITES [25] are interferometric methods that measure the full spatiotemporal structure of a collimated pulsed beam, from which the Fourier-limited space-time couplings can be calculated. INSIGHT [26] is a related technique designed to work in the vicinity of a beam focus, but it measures a strongly attenuated replica of a high-intensity beam. All these spatiotemporal methods also require an independent (and *ex situ*) temporal measurement of the pulse obtained from a self-referenced technique such as FROG, SPIDER, or d-scan.

HHG d-scan [27] uses the sensitivity of the HHG XUV signal itself to extract the second- and third-order phases of the intense laser pulse in a d-scan type measurement. However, this is inadequate for performing an accurate measurement of a few-cycle pulse or an ultrashort pulse with a more complex phase. This method also requires measurements of the high harmonic radiation, hindering its use as a parallel online diagnostic. More closely related to the present study is the recently published work by Leshchenko *et al.* [28] that describes an *in situ* pulse diagnostic applicable to laser–solid interactions at the lower edge of the relativistic intensity range. It is based on a dispersion-scan type measurement using the relativistic surface second harmonic (SH). To achieve the over-dense plasma at the target surface necessary for the SH mechanism ("oscillating mirror" [29]), a prepulse at $\approx 10^{15}\,\mathrm{Wcm}^{-2}$ was used with an adjustable delay relative to the pulse to be measured, to optimize the pre-plasma gradient to which the performance of relativistic SH is very sensitive. By successively inserting different pieces of dispersive material into the beam, d-scan measurements could be performed using the SH radiation. On-target pulse retrievals of 6 fs pulses (central wavelength 900 nm) were achieved for a pulse intensity of $\approx 1.7 \times 10^{18}\,\mathrm{Wcm}^{-2}$, corresponding to a normalized vector potential $a_0 \approx 1$. Supporting measurements and particle-in-cell simulations revealed that the scaling of the relativistic SH signal on laser intensity begins to saturate for $a_0 \gtrapprox 1$, hindering accurate pulse retrievals above this intensity.

In the present work, we demonstrate a new all-optical, *in situ* measurement method based on a third harmonic (TH) d-scan [30–32] that does not require an additional pulse. It is applicable to both gaseous and solid target interactions since it is based on a third-order nonlinear optical process and thus is not subject to the inversion symmetry constraints of SHG. Another advantage of a TH-based diagnostic compared to SHG is an increased spectral separation from the fundamental spectrum, which is advantageous from a signal-to-noise perspective (it is common for the spectrum of a few-cycle pulse to overlap with its SH spectrum). The TH generation (THG) has been observed over a very wide intensity range, from $4 \times 10^{9}\,\mathrm{Wcm}^{-2}$ from nanostructured metasurfaces [33] of interest for strong-field interactions due to their field-enhancement properties [34], to relativistic intensities of $10^{18} - 10^{21}\,\mathrm{Wcm}^{-2}$ [35,36]. In this paper, we focus on the $10^{13} - 10^{15}\,\mathrm{Wcm}^{-2}$ intensity range [37,38], where THG inevitably accompanies a variety of important strong-field processes, such as multiphoton- and tunnel-ionization and HHG. Previous works in this intensity range [39–41] have shown that the generated TH has a simple cubic (perturbative) scaling with laser intensity, eliminating the need for supporting intensity-scaling measurements. This cubic scaling appears to hold for a broad range of wavelengths from the deep ultraviolet [40] to the mid-infrared [41]. Collectively, these features of the TH make it ideally suited as a general-purpose *in situ* dynamical probe to accompany strong-field experiments.

We shall subsequently refer to this new technique as THIS: d-scan (third harmonic in-situ d-scan). Like almost all other pulse diagnostics, it cannot retrieve the CEP, although in situations where the intense pulses have extremely broad bandwidths [42], the resulting overlap between TH and fundamental spectra should enable measuring the CEP stability [43] or retrieving the full optical field and absolute CEP *in situ* [44]. For HHG driven by few-cycle pulses in gas-jets, the CEP can be sufficiently resolved from a parallel HHG measurement [45], which this technique allows.

In our present HHG experiments, THIS:d-scan was implemented by sampling the TH of the laser that is always generated in the gas target at the same time as high harmonics are generated. By directing the TH out of the chamber and recording its spectrum as a function of dispersion introduced onto the laser beam by the existing pulse compressor in the laser system, a d-scan measurement can be made. In cases such as for our experiment, where the target thickness is small compared to the confocal parameter of the focused laser beam, the generation volumes for the TH and high harmonics will overlap, ensuring the laser pulse is measured in the HHG interaction region. We show that this new method is capable of accurately characterizing intense pulses of 4 fs in duration under conditions optimized for HHG.

2. EXPERIMENTAL DETAILS

The experimental setup is shown in Fig. 1. Laser pulses of 25 fs duration and 2 mJ energy from a Ti:sapphire laser amplifier

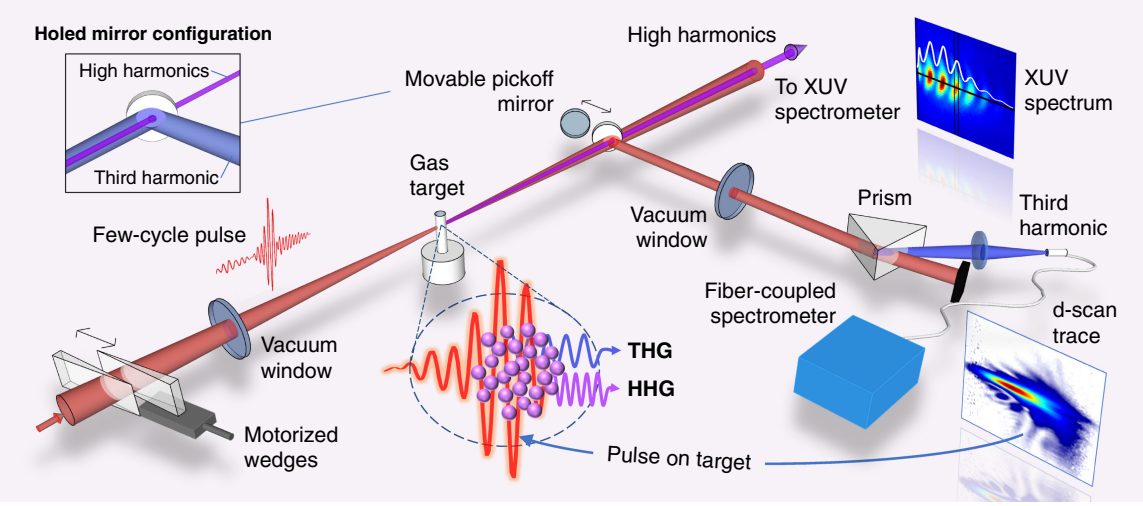

Fig. 1. Schematic of our experimental implementation of THIS:d-scan. 4 fs pulses centered at 800 nm from a hollow-fiber plus chirped-mirror compressor system were (entering at lower left of figure) passed through a motorized wedge pair for dispersion control and then into a vacuum beamline via a thin fused-silica window. The pulses were focused to around 10^{14} Wcm^{-2} into a gas tube target to generate high harmonics (HHs) and also the third harmonic (TH). Focusing was achieved with a spherical mirror (not shown in the figure for clarity) inside the chamber used at a low angle of incidence. The HHs propagated to an XUV spectrometer, where their spatially dependent spectra were recorded with a microchannel plate detector. An aluminum-coated pickoff mirror on a motorized translation stage was used to intercept the beam after the gas target to steer the TH out of the chamber where its spectrum was measured using a compact fiber-coupled spectrometer. The HHs are blocked by the exit vacuum window. The TH was separated from the 800 nm fundamental beam using a prism pair (for clarity, only one prism is shown). The TH spectrum was recorded as a function of wedge insertion to obtain the d-scan trace, which provides an *in situ* characterization of the 4 fs pulse in the gas target. The inset in the top left of the figure shows an alternate geometry where a holed (stationary) mirror is used to sample the TH for an online measurement, taking advantage of the lower divergence of the HHs.

(Femtolasers Femtopower) operating at a wavelength of 800 nm and a pulse repetition rate of 1 kHz were passed through a Ne-filled hollow core fiber [46,47] (1 m in length, 250 μm inner diameter, differentially pumped with 3 bar of Ne supplied to the fiber output and vacuum maintained at the fiber input). This caused the spectrum of the pulses to be broadened by a factor of ≈6. These positively chirped pulses were then sent through a chirped mirror compressor (550–1000 nm) to be temporally compressed. Near transform-limited pulses <4 fs in duration were generated by fine-tuning the dispersion using a pair of BaK5 glass wedges. Pulse energies up to 1 mJ were achieved.

For this experiment, these pulses with energies reduced to <0.3 mJ were sent through a 0.5-mm-thick fused-silica window into a vacuum beamline [46], where they were focused by a 50 cm focal length silver-coated mirror into a gas target to generate high-order harmonics. The beam waist radius was ≈100 μm. The gas target is of a standard design [46]. It consists of a thin-walled metal tube pressurized with gas (Ne or Ar in this work). Two small laser-drilled holes in the tube walls permitted the focused laser beam to pass through the gas contained within the tube, while limiting gas leakage into the chamber. The gas interaction length was estimated to be around 1 mm.

The high harmonics were spectrally dispersed and detected by an XUV spectrometer with an imaging microchannel plate detector, read out by a charged coupled-device camera. An aluminum-coated mirror inside the vacuum chamber could be moved into the beam after the gas target to send the laser beam and low-order harmonics out of the chamber through a calcium fluoride window. The TH was filtered from this beam using a pair of Brewster angle fused silica prisms (both prisms having an apex angle of 69°) in a retro-reflection geometry (to cancel spatial chirp) and analyzed with a compact fiber-coupled spectrometer (Ocean Optics HR4000). An obvious extension of this proof-of-concept setup, as shown in the inset in Fig. 1, is to use a pick-off mirror for the TH with a hole in it to reflect a portion of the TH, while allowing the lower-divergence high harmonics to pass through. This allows the laser pulse to be measured at the same time as HHG, hence providing an online, on-target measurement. A flip-mirror positioned before the entrance window of the vacuum chamber enabled the compressed laser pulse to be alternately sent to a home-built spatially encoded SPIDER variant (SEA-F-SPIDER) [48] to provide an independent pulse characterization and to obtain a reference pulse (i.e., before it passes through the vacuum chamber window and is focused into the gas target).

The THIS:d-scan measurement was first performed by recording the TH spectrum in Ar (and later in Ne) as a function of dispersion by scanning the glass wedges used for compression optimization around their optimal compression position. A full dispersion scan with small dispersion steps, such as this, allows for higher-quality d-scan retrievals [49] compared to a discrete dispersion scan from inserting pieces of dispersive material [28]. We scanned the dispersion in 128 steps of 2 fs^2 at 800 nm (512 steps of 0.5 fs^2 in Ne), corresponding to a total insertion of one of the wedges of ≈4.5 mm. The wedge was moved using a motorized translation stage, and the spectrometer signal was averaged over two laser pulses (five laser pulses in Ne) at each dispersion point. The acquisition was synchronized with the repetition rate of the laser pulses via a trigger signal from the amplifier. An entire scan took approximately 10 s (100 s for Ne).

3. RESULTS AND DISCUSSION

The d-scan traces recorded in an Ar gas target at a pressure of 100 mbar are shown in Fig. 2(b). The laser pulse energy was

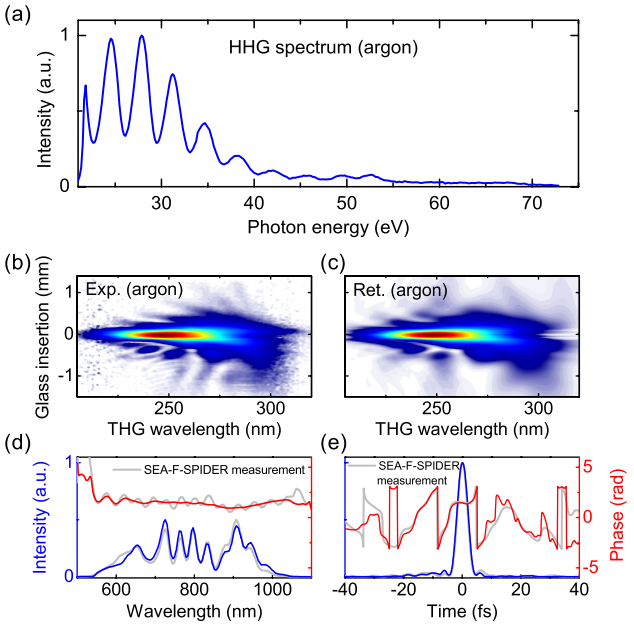

Fig. 2. Data obtained with Ar as the HHG nonlinear medium. (a) HHG spectrum, (b) measured TH d-scan trace, (c) retrieved d-scan trace, (d) reconstructed spectrum and spectral phase with comparison to the SEA-F-SPIDER measurement, (e) reconstructed pulse profile and temporal phase with comparison to the SEA-F-SPIDER measurement.

0.13 mJ, and the on-target peak intensity was estimated to be 2×10^{14} Wcm^{-2}. This is in agreement with the peak intensity calculated from the ≈55 eV cutoff in the Ar HHG spectrum shown in Fig. 2(a) using the $I_p + 3.2U_p$ rule [50,51] for the cutoff energy, where I_p is the ionization potential of the gas atoms, and U_p is the ponderomotive potential of the focused laser beam. The Ar HHG spectrum was recorded under identical conditions to the d-scan measurement by simply moving the TH pick off mirror out of the beam path.

For the d-scan retrieval, we assumed a simple cubic dependence of the TH field on the laser field, as expected for a gas-jet (thin target) under low-ionization conditions [37,39,41]. If we consider a pulse in the frequency domain, $\tilde{E}(\omega) = |\tilde{E}(\omega)|e^{i\varphi(\omega)}$, where ϕ is the spectral phase, the measured d-scan trace, S_{meas}, can be written as the product of a spectral response function, $R(\omega)$, accounting for a non-instantaneous nonlinearity and spectral filtering in the measurement and an ideal trace, S_{ideal} [4]:

$$S_{\text{meas}} = R(\omega) \quad S_{\text{ideal}} \equiv R(\omega)\left|\int_{-\infty}^{+\infty} E_{\text{NL}} e^{-i\omega t} \mathrm{d}t\right|^2, \qquad (1)$$

where E_{NL} is the dispersion-dependent nonlinear signal. For THIS:d-scan, E_{NL} will be given by the cube of the time-domain field on target, $E(t, \zeta)$, normalized by an amplitude factor, $A(t, \zeta) = |E(t, \zeta)|^{n-3}$, to account for a power dependence, n, of the TH signal on the laser intensity other than the third, i.e.,

$$E_{\text{NL}} = A\, E^3(t, \zeta) \propto A\left(\int_{-\infty}^{+\infty} \tilde{E}(\Omega) e^{-i\beta(\Omega)\zeta} e^{i\Omega t} \mathrm{d}\Omega\right)^3, \qquad (2)$$

with $\beta(\Omega)$ the frequency-dependent phase per unit displacement introduced by the compressor and ζ the compressor position. In the present experiments, we assume $n \approx 3$, and hence, we set $A(t, \zeta) = 1$.

An advanced full d-scan retrieval [52] variant was implemented, which retrieves both the full electric field of the pulse, $\tilde{E}(\omega)$, and the unknown response function, $R(\omega)$, without input of the laser spectrum from another measurement nor intensity calibration of the measured TH signal. The spectrum and spectral phase are therefore retrieved from the d-scan trace alone, in a fully *in situ* manner. The traces were interpolated onto a 128 × 512 matrix (insertion × wavelength), and the phase was parameterized using all 512 wavelength points as free variables. The retrievals took a few seconds on a standard laptop computer.

The retrieved d-scan trace is in good agreement with the measured trace (d-scan retrieval error [4] of 0.4%). Figure 2(d) shows the retrieved laser pulse spectrum and spectral phase. The pulse profile and temporal phase are shown in Fig. 2(e). Also shown in these figures is the pulse reconstruction from the SEA-F-SPIDER diagnostic, which measured the pulse before the vacuum chamber. The agreement is excellent, considering that the measurements were performed using two very different techniques, based on different-order nonlinearities, and in very different nonlinear media (*in situ* THG in a gas-jet for THIS:d-scan versus *ex situ* SFG in a nonlinear crystal for SEA-F-SPIDER). All peaks in the spectrum are closely matched, and the widths of the temporal profile are the same (4.0 ± 0.1 fs for d-scan and 3.90 ± 0.06 fs for SPIDER) within the experimental uncertainty. Even the small pre- and post-pulses on the temporal profile (all below 4% of the main peak) are matching in both reconstructions. The spectral phase measured by THIS:d-scan is significantly smoother than that measured by SEA-F-SPIDER, but it shows the same general behavior.

A single THIS:d-scan measurement contains all possible pulse shapes achievable with the compressor over the measurement scan range [4], which presents an important practical and technical advantage. Measurements of HHG (or other strong-field processes) performed for any position of the compressor can be perfectly matched up with the corresponding shape and phase of the driving laser pulse directly on target and without the need for additional measurements. In the present experiments, this allowed us to confirm that the maximum HHG yield occurs for the wedge insertion that indeed gives the shortest and more intense pulse on target—defined as the "zero" glass insertion in Figs. 2(b) and 2(c)—but this capability is also particularly relevant for coherent control of HHG and other strong-field processes employing shaped (e.g., chirped [53,54]) laser pulses.

We note that the low retrieval error and the excellent agreement between THIS:d-scan and SEA-F-SPIDER measurements provide further evidence for a perturbative cubic dependence of the TH on the laser field, even in a situation where laser intensities are clearly in the non-perturbative regime and can excite strong-field processes such as HHG.

We then changed from Ar to Ne in the gas target and repeated the measurement. The Ne pressure was ≈300 mbar, and the laser pulse energy increased to 0.26 mJ, resulting in an estimated on-target peak intensity of 4×10^{14} Wcm^{-2}, again consistent with the ≈100 eV cutoff energy in the Ne HHG spectrum, as shown in Fig. 3(a).

Figures 3(b) and 3(c) show the measured and retrieved d-scan traces using THG in Ne. The retrieval (512 × 512 matrix; d-scan error of 0.5%) is not as a good as in Ar. This is due to a significantly lower TH signal in Ne compared to Ar (χ_3(Ne) ≈ χ_3(Ar)/13 [55]), which reduced the signal-to-noise ratio (SNR) of the

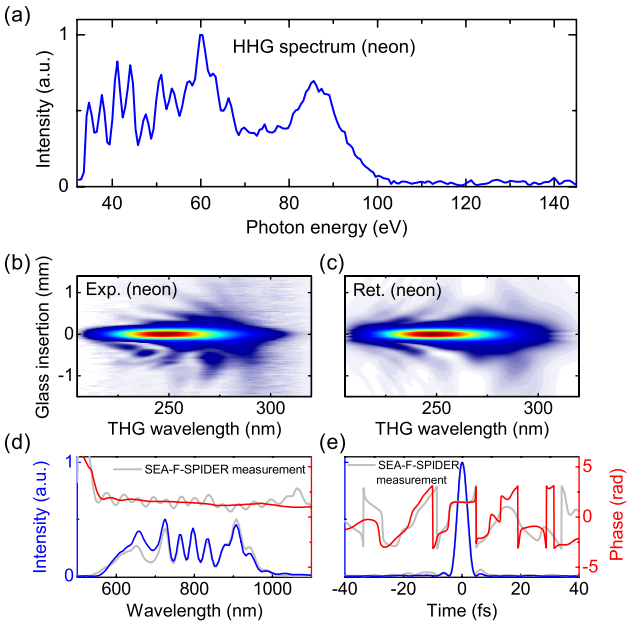

Fig. 3. Data obtained with Ne as the HHG nonlinear medium. (a) HHG spectrum, (b) measured TH d-scan trace, (c) retrieved d-scan trace, (d) reconstructed spectrum and spectral phase with comparison to the SEA-F-SPIDER measurement, (e) reconstructed pulse profile and temporal phase with comparison to the SEA-F-SPIDER measurement.

measurement. The comparison between the THIS:d-scan and SEA-F-SPIDER pulse reconstructions is shown in Figs. 3(e) and 3(f). Despite the poorer d-scan retrieval, the laser spectrum is reasonably well reconstructed, with the largest difference between the SEA-F-SPIDER spectrum at the blue end. While it is most likely that this is a SNR issue, it is possible that the difference is a consequence of some slight spectral reshaping of the pulse in the gas target [56] (see later for further discussion). As with Ar, the THIS:d-scan phase appears to be a smoothed version of the SEA-F-SPIDER's. The pulse profiles are still extremely similar and have the same width (4.0 ± 0.1 fs for d-scan and 3.90 ± 0.06 fs for SPIDER) within the experimental uncertainty, with similar small satellite pulses in both measurements. The observed smoothing in the spectral phase is likely due to the stronger intensity dependence of third-order processes compared to second-order ones, which makes weak pulses that are temporally well-separated from the main peak (i.e, those due to rapid phase oscillations) harder to detect. This results in d-scan traces that appear less structured than their second-order counterparts for the same dynamic range in signal intensity [32], but still enable accurate pulse measurements down to a single cycle [32,57].

4. PERSPECTIVES

Most HHG experiments are carried out under conditions of low ionization and low-target density [58–60]. This is because high levels of ionization lead to a reduction in the efficiency due to ground-state depletion and degraded phase-matching owing to the high dispersion of free electrons. The latter effect is compounded by increasing gas density. Typically for HHG, $\eta p L < \approx 5$ mbar.mm, where η is the fraction of atoms ionized, p is the gas target pressure, and L is its length. For example, in this work, $L \approx 1$ mm, $p < 300$ mbar, $I_0 \approx 2 \times 10^{14}$, and 4×10^{14} Wcm^{-2} for Ar and Ne, respectively. For these intensities, η, which we calculated using laser-tunneling ionization rates [61], is <1% for both gases, and hence $\eta p L < 3$ mbar.mm. Under these conditions, distortion of the laser pulse due to propagation through the gas target is negligible. This can be appreciated by considering the group-delay dispersion (GDD) of the partially ionized gas target, which at $\lambda \approx 800$ nm is given by $\mathrm{GDD}_{\mathrm{target}} \approx -\eta(p/\mathrm{mbar})(L/\mathrm{mm}) \times 0.02\ \mathrm{fs}^2$. This formula is based on the dispersion of the free electrons, which is more than an order of magnitude greater than neutral gas dispersion for $\eta \gtrsim 1\%$. For our parameters, $\mathrm{GDD}_{\mathrm{target}} < -0.06\ \mathrm{fs}^2$, which is the equivalent to ≈ 1.5 μm of fused silica and causes negligible pulse broadening to a 4 fs pulse. This explains the close agreement between the THIS:d-scan pulse measurement and the *ex situ* SEA-F-SPIDER measurement.

However, there is growing interest [62–64] in HHG beyond the conventional weak-plasma limit. Recently, an order-of-magnitude increase in harmonic flux in the water-window (285–540 eV range) was demonstrated by pushing the experimental parameters beyond this limit [62]. This was achieved by using a very high pressure gas target, with $p \approx 10$ bar, and employing a higher-than-usual laser intensity ($>2 \times 10^{15}$ Wcm^{-2} in Ne), which although clamped to a somewhat lower level lead to an ionization fraction approaching 10%. For these parameter values, $\eta p L \approx 10^3$ mbar.mm, almost three orders of magnitude higher than the value attained in the present work. Simulations in [62] revealed a strong reshaping of the laser pulse as it propagated through the gas target and showed that this reshaping was key to the increased harmonic efficiency and extended cutoff. Although we could not access this regime in the present work due to limitations of our gas target density, we expect that for such situations, where $\eta p L \gg 10$ mbar.mm, THIS:d-scan can provide evidence that pulse reshaping is taking place, since effects such as dispersive pulse broadening should result in stretched traces along the dispersion axis and longer retrieved pulses compared to the low-dispersion regime, as demonstrated for the third-order d-scan using thick crystals [57]. Exact quantification of the reshaping in this regime will require adapting the algorithm to include pulse propagation within the target [57]. The ability to make such a measurement is important to validate simulations and to enable the optimization of experimental conditions in this strong-plasma regime, e.g., to maximize the harmonic flux at very high photon energy.

The THIS:d-scan technique can be extended to experiments involving longer pulses, such as those produced directly by chirped pulse amplification (CPA) systems. In these cases, the compressor within the laser system itself (or any suitable pulse compressor) can be varied to provide the required scan for the on-target measurement [65,66], without the need for additional elements or pulse compressors. Knowledge of the nominal dispersion of the compressor is not necessary in principle, since the d-scan algorithm can also retrieve it, as demonstrated for SH d-scan with <30 fs pulses [66].

In the particular case of ultra-high intensity CPA lasers in the multi-TW to PW range, the TH emission accompanying strong-plasma processes in solid targets can exhibit a well-behaved and approximately linear dependence on the incident laser intensity over a very broad intensity range, from 10^{16} Wcm^{-2} to at least 10^{21} Wcm^{-2} [35]. Imaging at the TH generated and reflected by the solid target provides a nearly noise-free window on the interaction, allowing accurate *in situ* measurement of the spatial energy distribution in the focal spot at full laser power, as demonstrated

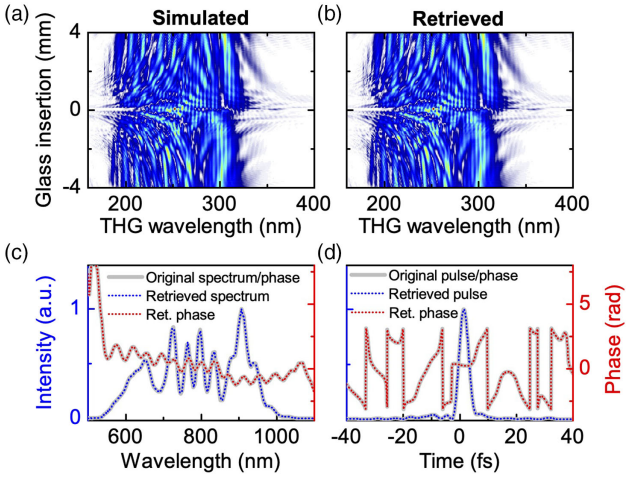

Fig. 4. Illustration of THIS:d-scan measurement in the relativistic regime (linear scaling of the TH signal with laser intensity, as expected for pulse peak intensities from 10^{18} to 10^{21} Wcm^{-2}). (a) Simulated TH d-scan trace, (b) retrieved d-scan trace, (c) reconstructed spectrum and spectral phase with comparison to the reference pulse, (e) reconstructed pulse profile and temporal phase with comparison to the reference pulse.

for a PW-level, 500 fs laser [35], and very recently for a multi-TW, <35 fs laser [36]. The characteristics of this TH emission appear highly favorable for the *in situ* temporal measurement of the ultra-intense driving laser pulses with THIS:d-scan, provided the appropriate scaling of the TH signal with laser intensity is built into the retrieval.

To illustrate the potential applicability of THIS:d-scan in this regime, we simulated a measurement and full retrieval of a few-cycle pulse with a peak intensity anywhere between 10^{18} to 10^{21} Wcm^{-2}, using $n = 1$ (linear scaling) in the amplitude factor of Eq. (2), which gives $|E_{\mathrm{NL}}| \propto |E(t, \zeta)|$, hence reproducing the TH behavior observed at relativistic intensities. For the simulations, we used a 200 × 1000 matrix (insertion × wavelength) and assumed BK7 glass wedges. The results are summarized in Fig. 4. We see that the linear scaling of the TH results in extended traces along the dispersion axis [Fig. 4(a)] compared to the simple cubic TH case [Figs. 2(a) and 3(a)], since in this regime, the total TH energy is independent of the laser pulse chirp over the whole scan range of the wedges (±4 mm around the maximum compression point). Nevertheless, the d-scan trace still encodes amplitude and phase information and can be fully retrieved [Fig. 4(b)]. The d-scan error was 0.1% (limited by numerical noise), and the pulse was retrieved without any ambiguities, as shown in Figs. 4(c) and 4(d).

In these extreme conditions, the target roughness can induce scattering of the TH emission [35], adding an incoherent component to the measured d-scan trace, but this type of process can be modelled and incorporated in the d-scan retrieval to accurately extract the laser pulse alone [67]. In gas targets, THIS:d-scan should enable the *in situ* measurement of relativistic driving laser pulses, including the few-cycle pulses used for laser wakefield electron acceleration at kHz repetition rates [13]. The emergence of a new generation of ultra-high power laser facilities around the world, with unprecedentedly high repetition rates and pulse stability parameters comparable to those of tabletop systems [68], enables the practical implementation of measurements and techniques that rely on a set of identical pulses, such as THIS:d-scan.

5. CONCLUSIONS

We have proposed and demonstrated a new technique, THIS:d-scan, based on a TH d-scan for the *in situ*, full characterization of ultrashort laser pulses. We demonstrated the technique by characterizing few-cycle pulses at their full power during HHG and validated our measurements using an independent pulse diagnostic. The technique could equally well be applied to other intense laser–matter interaction experiments requiring ultrashort laser pulses. The setup for THIS:d-scan can be easily added to an existing beamline at relatively low cost and provides a pulse characterization at the location of the sample, thus eliminating the need for the error-prone process of attempting to equalize optical path lengths, which is necessary with *ex situ* measurements. Furthermore, it provides an accurate measurement of the pulse directly on target, including any linear or nonlinear phase acquired within the beamline and possibly the target itself. For HHG in the conventional weak-plasma regime, we have shown that THIS:d-scan gives excellent agreement with an *ex situ* measurement made by a SEA-F-SPIDER diagnostic. The retrieved pulse durations are the same within the experimental uncertainty, and matching small features in the spectrum and pulse profile are seen in both measurements. The fact that the TH emission, unlike the SH emission, occurs in gases, solids, and plasmas over a broad range of target densities, pulse durations and laser intensities extending well into the relativistic regime, makes THIS:d-scan a very promising technique for the *in situ* temporal characterization of ultrashort laser pulses during strong-field laser–matter interaction at the extreme conditions presently attainable with ultra-high power lasers.

Funding. Engineering and Physical Sciences Research Council (EP/I032517/1); Defence Science and Technology Laboratory (EP/N018680/1); Fundação para a Ciência e a Tecnologia (M-ERA-NET2/0002/2016, PTDC/FIS-OTI/32213/2017, UIDB/04968/2020); Programa Operacional Temático Factores de Competitividade (NORTE-01-0145-FEDER-022096).

Acknowledgment. The authors thank F. Silva, A. Gregory, C. O'Donovan, and S. Parker for technical support.

Disclosures. HC: Sphere Ultrafast Photonics (I,P,S), MM: Sphere Ultrafast Photonics (I,E,P).

REFERENCES

1. R. Trebino, K. W. DeLong, D. N. Fittinghoff, J. N. Sweetser, M. A. Krumbügel, B. A. Richman, and D. J. Kane, "Measuring ultrashort laser pulses in the time-frequency domain using frequency-resolved optical gating," Rev. Sci. Instrum. **68**, 3277–3295 (1997).
2. C. Iaconis and I. A. Walmsley, "Spectral phase interferometry for direct electric-field reconstruction of ultrashort optical pulses," Opt. Lett. **23**, 792–794 (1998).
3. V. V. Lozovoy, I. Pastirk, and M. Dantus, "Multiphoton intrapulse interference. IV. Ultrashort laser pulse spectral phase characterization and compensation," Opt. Lett. **29**, 775–777 (2004).
4. M. Miranda, T. Fordell, C. Arnold, A. L'Huillier, and H. Crespo, "Simultaneous compression and characterization of ultrashort laser pulses using chirped mirrors and glass wedges," Opt. Express **20**, 688–697 (2012).
5. M. Nisoli, S. D. Silvestri, O. Svelto, R. Szipöcs, K. Ferencz, C. Spielmann, S. Sartania, and F. Krausz, "Compression of high-energy laser pulses below 5 fs," Opt. Lett. **22**, 522–524 (1997).

6. T. Brabec and F. Krausz, "Intense few-cycle laser fields: frontiers of nonlinear optics," Rev. Mod. Phys. **72**, 545–591 (2000).
7. J. Rothhardt, S. Hädrich, J. Delagnes, E. Cormier, and J. Limpert, "High average power near-infrared few-cycle lasers," Laser Photon. Rev. **11**, 1700043 (2017).
8. F. Silva, B. Alonso, W. Holgado, R. Romero, J. S. Román, E. C. Jarque, H. Koop, V. Pervak, H. Crespo, and I. J. Sola, "Strategies for achieving intense single-cycle pulses with in-line post-compression setups," Opt. Lett. **43**, 337–340 (2018).
9. F. Krausz and M. Ivanov, "Attosecond physics," Rev. Mod. Phys. **81**, 163–234 (2009).
10. D. Fabris, T. Witting, W. A. Okell, D. J. Walke, P. Matia-Hernando, J. Henkel, T. R. Barillot, M. Lein, J. P. Marangos, and J. W. G. Tisch, "Synchronized pulses generated at 20 eV and 90 eV for attosecond pump–probe experiments," Nat. Photonics **9**, 383–387 (2015).
11. S. Ghimire and D. A. Reis, "High-harmonic generation from solids," Nat. Phys. **15**, 10–16 (2019).
12. K. Schmid, L. Veisz, F. Tavella, S. Benavides, R. Tautz, D. Herrmann, A. Buck, B. Hidding, A. Marcinkevicius, U. Schramm, M. Geissler, J. M. Vehn, D. Habs, and F. Krausz, "Few-cycle laser-driven electron acceleration," Phys. Rev. Lett. **102**, 124801 (2009).
13. D. Guénot, D. Gustas, A. Vernier, B. Beaurepaire, F. Böhle, M. Bocoum, M. Lozano, A. Jullien, R. Lopez-Martens, A. Lifschitz, and J. Faure, "Relativistic electron beams driven by kHz single-cycle light pulses," Nat. Photonics **11**, 293–296 (2017).
14. J. Faure, D. Gustas, D. Guénot, A. Vernier, F. Böhle, M. Ouillé, S. Haessler, R. Lopez-Martens, and A. Lifschitz, "A review of recent progress on laser-plasma acceleration at kHz repetition rate," Plasma Phys. Controlled Fusion **61**, 014012 (2018).
15. E. Goulielmakis, M. Uiberacker, R. Kienberger, A. Baltuska, V. Yakovlev, A. Scrinzi, T. Westerwalbesloh, U. Kleineberg, U. Heinzmann, M. Drescher, and F. Krausz, "Direct measurement of light waves," Science **305**, 1267–1269 (2004).
16. T. Witting, F. Frank, W. A. Okell, C. A. Arrell, J. P. Marangos, and J. W. G. Tisch, "Sub-4-fs laser pulse characterization by spatially resolved spectral shearing interferometry and attosecond streaking," J. Phys. B **45**, 074014 (2012).
17. A. Blättermann, C. Ott, A. Kaldun, T. Ding, V. Stooß, M. Laux, M. Rebholz, and T. Pfeifer, "In situ characterization of few-cycle laser pulses in transient absorption spectroscopy," Opt. Lett. **40**, 3464–3467 (2015).
18. A. S. Wyatt, T. Witting, A. Schiavi, D. Fabris, P. Matia-Hernando, I. A. Walmsley, J. P. Marangos, and J. W. G. Tisch, "Attosecond sampling of arbitrary optical waveforms," Optica **3**, 303–310 (2016).
19. K. T. Kim, C. Zhang, A. D. Shiner, B. E. Schmidt, F. Légaré, D. M. Villeneuve, and P. B. Corkum, "Petahertz optical oscilloscope," Nat. Photonics **7**, 958–962 (2013).
20. S. B. Park, K. Kim, W. Cho, S. I. Hwang, I. Ivanov, C. H. Nam, and K. T. Kim, "Direct sampling of a light wave in air," Optica **5**, 402–408 (2018).
21. A. J. Verhoef, A. Mitrofanov, A. Zheltikov, and A. Baltuška, "Plasma-blueshift spectral shear interferometry for characterization of ultimately short optical pulses," Opt. Lett. **34**, 82–84 (2009).
22. B. Alonso, I. J. Sola, Ó. Varela, J. Hernández-Toro, C. Méndez, J. S. Román, A. Zaïr, and L. Roso, "Spatiotemporal amplitude-and-phase reconstruction by Fourier-transform of interference spectra of high-complex-beams," J. Opt. Soc. Am. B **27**, 933–940 (2010).
23. B. Alonso, M. Miranda, F. Silva, V. Pervak, J. Rauschenberger, J. San Román, Í. J. Sola, and H. Crespo, "Characterization of sub-two-cycle pulses from a hollow-core fiber compressor in the spatiotemporal and spatiospectral domains," Appl. Phys. B **112**, 105–114 (2013).
24. M. Miranda, M. Kotur, P. Rudawski, C. Guo, A. Harth, A. L'Huillier, and C. L. Arnold, "Spatiotemporal characterization of ultrashort laser pulses using spatially resolved Fourier transform spectrometry," Opt. Lett. **39**, 5142–5145 (2014).
25. G. Pariente, V. Gallet, A. Borot, O. Gobert, and F. Quéré, "Space–time characterization of ultra-intense femtosecond laser beams," Nat. Photonics **10**, 547–553 (2016).
26. A. Borot and F. Quéré, "Spatio-spectral metrology at focus of ultrashort lasers: a phase-retrieval approach," Opt. Express **26**, 26444–26461 (2018).
27. D. S. Brambila, A. Husakou, M. Ivanov, and N. Zhavoronkov, "On-target diagnosing of few-cycle pulses by high-order-harmonic generation," Phys. Rev. A **96**, 063825 (2017).
28. V. E. Leshchenko, A. Kessel, O. Jahn, M. Krüger, A. Münzer, S. A. Trushin, L. Veisz, Z. Major, and S. Karsch, "On-target temporal characterization of optical pulses at relativistic intensity," Light Sci. Appl. **8**, 96 (2019).
29. T. Baeva, S. Gordienko, and A. Pukhov, "Theory of high-order harmonic generation in relativistic laser interaction with overdense plasma," Phys. Rev. E **74**, 046404 (2006).
30. F. Silva, M. Miranda, S. Teichmann, M. Baudish, M. Massicotte, F. Koppens, J. Biegert, and H. Crespo, "Near to mid-IR ultra-broadband third harmonic generation in multilayer graphene: few-cycle pulse measurement using THG dispersion-scan," in *Conference on Lasers and Electro-Optics (CLEO)* (Optical Society of America, 2013), paper CW1H.5.
31. M. Hoffmann, T. Nagy, T. Willemsen, M. Jupé, D. Ristau, and U. Morgner, "Pulse characterization by THG d-scan in absorbing nonlinear media," Opt. Express **22**, 5234–5240 (2014).
32. M. Canhota, F. Silva, R. Weigand, and H. M. Crespo, "Inline self-diffraction dispersion-scan of over octave-spanning pulses in the single-cycle regime," Opt. Lett. **42**, 3048–3051 (2017).
33. M. Semmlinger, M. Zhang, M. L. Tseng, T.-T. Huang, J. Yang, D. P. Tsai, P. Nordlander, and N. J. Halas, "Generating third harmonic vacuum ultraviolet light with a TiO_2 metasurface," Nano Lett. **19**, 8972–8978 (2019).
34. H. Liu, C. Guo, G. Vampa, J. L. Zhang, T. Sarmiento, M. Xiao, P. H. Bucksbaum, J. Vučković, S. Fan, and D. A. Reis, "Enhanced high-harmonic generation from an all-dielectric metasurface," Nat. Phys. **14**, 1006–1010 (2018).
35. B. Dromey, C. Bellei, D. Carroll, R. Clarke, J. Green, S. Kar, S. Kneip, K. Markey, S. Nagel, L. Willingale, P. McKenna, D. Neely, Z. Najmudin, K. Krushelnick, P. A. Norreys, and M. Zepf, "Third harmonic order imaging as a focal spot diagnostic for high intensity laser-solid interactions," Laser Part. Beams **27**, 243–248 (2009).
36. D. Raffestin, G. Boutoux, N. Blanchot, D. Batani, E. D'Humières, Q. Moreno, T. Longhi, H. Covïc, F. Granet, J. Rault, C. Liberatore, K. Jakubowska, and V. Tikhonchuk, "Application of harmonics imaging to focal spot measurements of the "petal" laser," J. Appl. Phys. **126**, 245902 (2019).
37. A. L'Huillier, L. A. Lompré, M. Ferray, X. F. Li, G. Mainfray, and C. Manus, "Third-harmonic generation in xenon in a pulsed jet and a gas cell," Europhys. Lett. **5**, 601–605 (1988).
38. R. A. Ganeev, M. Suzuki, M. Baba, H. Kuroda, and I. A. Kulagin, "Third-harmonic generation in air by use of femtosecond radiation in tight-focusing conditions," Appl. Opt. **45**, 748–755 (2006).
39. U. Graf, M. Fieß, M. Schultze, R. Kienberger, F. Krausz, and E. Goulielmakis, "Intense few-cycle light pulses in the deep ultraviolet," Opt. Express **16**, 18956–18963 (2008).
40. H. Zhou, W. Li, L. Shi, D. Wang, L. Ding, and H. Zeng, "Efficient generation of vacuum and extreme ultraviolet pulses," Laser Phys. Lett. **11**, 025402 (2014).
41. J. Ni, J. Yao, B. Zeng, W. Chu, G. Li, H. Zhang, C. Jing, S. L. Chin, Y. Cheng, and Z. Xu, "Comparative investigation of third- and fifth-harmonic generation in atomic and molecular gases driven by midinfrared ultrafast laser pulses," Phys. Rev. A **84**, 063846 (2011).
42. J. C. Travers, T. F. Grigorova, C. Brahms, and F. Belli, "High-energy pulse self-compression and ultraviolet generation through soliton dynamics in hollow capillary fibres," Nat. Photonics **13**, 547–554 (2019).
43. F. Silva, M. Miranda, B. Alonso, J. Rauschenberger, V. Pervak, and H. Crespo, "Simultaneous compression, characterization and phase stabilization of GW-level 1.4 cycle VIS-NIR femtosecond pulses using a single dispersion-scan setup," Opt. Express **22**, 10181–10191 (2014).
44. M. Miranda, F. Silva, L. Neoričić, C. Guo, V. Pervak, M. Canhota, A. S. Silva, I. J. Sola, R. Romero, P. T. Guerreiro, A. L'Huillier, C. L. Arnold, and H. Crespo, "All-optical measurement of the complete waveform of octave-spanning ultrashort light pulses," Opt. Lett. **44**, 191–194 (2019).
45. C. A. Haworth, L. E. Chipperfield, J. S. Robinson, P. L. Knight, J. P. Marangos, and J. W. G. Tisch, "Half-cycle cutoffs in harmonic spectra and robust carrier-envelope phase retrieval," Nat. Phys. **3**, 52–57 (2007).
46. F. Frank, C. Arrell, T. Witting, W. A. Okell, J. McKenna, J. S. Robinson, C. A. Haworth, D. Austin, H. Teng, I. A. Walmsley, J. P. Marangos, and J. W. G. Tisch, "Invited review article: technology for attosecond science," Rev. Sci. Instrum. **83**, 071101 (2012).
47. W. A. Okell, T. Witting, D. Fabris, D. Austin, M. Bocoum, F. Frank, A. Ricci, A. Jullien, D. Walke, J. P. Marangos, R. Lopez-Martens, and J. W. G. Tisch, "Carrier-envelope phase stability of hollow fibers used

for high-energy few-cycle pulse generation," Opt. Lett. **38**, 3918–3921 (2013).
48. T. Witting, F. Frank, C. A. Arrell, W. A. Okell, J. P. Marangos, and J. W. G. Tisch, "Characterization of high-intensity sub-4-fs laser pulses using spatially encoded spectral shearing interferometry," Opt. Lett. **36**, 1680–1682 (2011).
49. N. C. Geib, R. Hollinger, E. Haddad, P. Herrmann, F. Légaré, T. Pertsch, C. Spielmann, M. Zürch, and F. Eilenberger, "Discrete dispersion scan setup for measuring few-cycle laser pulses in the mid-infrared," arXiv:2004.12145 (2020).
50. J. L. Krause, K. J. Schafer, and K. C. Kulander, "High-order harmonic generation from atoms and ions in the high intensity regime," Phys. Rev. Lett. **68**, 3535–3538 (1992).
51. P. B. Corkum, "Plasma perspective on strong field multiphoton ionization," Phys. Rev. Lett. **71**, 1994–1997 (1993).
52. M. Miranda, J. Penedones, C. Guo, A. Harth, M. Louisy, L. Neoričić, A. L'Huillier, and C. L. Arnold, "Fast iterative retrieval algorithm for ultrashort pulse characterization using dispersion scans," J. Opt. Soc. Am. B **34**, 190–197 (2017).
53. F. Quéré, C. Thaury, J.-P. Geindre, G. Bonnaud, P. Monot, and P. Martin, "Phase properties of laser high-order harmonics generated on plasma mirrors," Phys. Rev. Lett. **100**, 095004 (2008).
54. W. Holgado, C. Hernández-García, B. Alonso, M. Miranda, F. Silva, L. Plaja, H. Crespo, and I. J. Sola, "Continuous spectra in high-harmonic generation driven by multicycle laser pulses," Phys. Rev. A **93**, 013816 (2016).
55. H. Lehmeier, W. Leupacher, and A. Penzkofer, "Nonresonant third order hyperpolarizability of rare gases and n_2 determined by third harmonic generation," Opt. Commun. **56**, 67–72 (1985).
56. W. Holgado, B. Alonso, J. S. Román, and I. J. Sola, "Temporal and spectral structure of the infrared pulse during the high order harmonic generation," Opt. Express **22**, 10191–10201 (2014).
57. A. Tajalli, M. Ouillé, A. Vernier, F. Böhle, E. Escoto, S. Kleinert, R. Romero, J. Csontos, U. Morgner, G. Steinmeyer, H. M. Crespo, R. L. Martens, and T. Nagy, "Propagation effects in the characterization of 1.5-cycle pulses by XPW dispersion scan," IEEE J. Sel. Top. Quantum Electron. **25**, 1–7 (2019).
58. P. Balcou, P. Salieres, A. L'Huillier, and M. Lewenstein, "Generalized phase-matching conditions for high harmonics: the role of field-gradient forces," Phys. Rev. A **55**, 3204–3210 (1997).
59. T. Popmintchev, M.-C. Chen, D. Popmintchev, P. Arpin, S. Brown, S. Ališauskas, G. Andriukaitis, T. Balčiunas, O. D. Mücke, A. Pugzlys, A. Baltuška, B. Shim, S. E. Schrauth, A. Gaeta, C. Hernández-Garca, L. Plaja, A. Becker, A. Jaron-Becker, M. M. Murnane, and H. C. Kapteyn, "Bright coherent ultrahigh harmonics in the keV X-ray regime from mid-infrared femtosecond lasers," Science **336**, 1287–1291 (2012).
60. C. M. Heyl, C. L. Arnold, A. Couairon, and A. L'Huillier, "Introduction to macroscopic power scaling principles for high-order harmonic generation," J. Phys. B **50**, 013001 (2016).
61. M. V. Ammosov, N. B. Delone, and V. P. Krainov, "Tunnel ionization of complex atoms and of atomic ions in an alternating electromagnetic field," Sov. Phys. JETP **64**, 1191–1194 (1987).
62. A. S. Johnson, D. R. Austin, D. A. Wood, C. Brahms, A. Gregory, K. B. Holzner, S. Jarosch, E. W. Larsen, S. Parker, C. S. Strüber, P. Ye, J. W. G. Tisch, and J. P. Marangos, "High-flux soft x-ray harmonic generation from ionization-shaped few-cycle laser pulses," Sci. Adv. **4**, eear3761 (2018).
63. C. Jin, M.-C. Chen, H.-W. Sun, and C. D. Lin, "Extension of water-window harmonic cutoff by laser defocusing-assisted phase matching," Opt. Lett. **43**, 4433–4436 (2018).
64. V. Cardin, B. E. Schimdt, N. Thiré, S. Beaulieu, V. Wanie, M. Negro, C. Vozzi, V. Tosa, and F. Légaré, "Self-channeled high harmonic generation of water window soft x-rays," J. Phys. B **51**, 174004 (2018).
65. V. Loriot, G. Gitzinger, and N. Forget, "Self-referenced characterization of femtosecond laser pulses by chirp scan," Opt. Express **21**, 24879–24893 (2013).
66. B. Alonso, Í. J. Sola, and H. Crespo, "Self-calibrating d-scan: measuring ultrashort laser pulses on-target using an arbitrary pulse compressor," Sci. Rep. **8**, 3264 (2018).
67. Ó. Pérez-Benito and R. Weigand, "Nano-dispersion-scan: measurement of sub-7-fs laser pulses using second-harmonic nanoparticles," Opt. Lett. **44**, 4921–4924 (2019).
68. C. N. Danson, C. Haefner, J. Bromage, T. Butcher, J.-C. F. Chanteloup, E. A. Chowdhury, A. Galvanauskas, L. A. Gizzi, J. Hein, D. I. Hillier, N. W. Hopps, Y. Kato, E. A. Khazanov, R. Kodama, G. Korn, R. Li, Y. Li, J. Limpert, J. Ma, C. H. Nam, D. Neely, D. Papadopoulos, R. R. Penman, L. Qian, J. J. Rocca, A. A. Shaykin, C. Siders, C. Spindloe, S. Szatmári, R. M. G. M. Trines, J. Zhu, P. Zhu, and J. Zuegel, "Petawatt and exawatt class lasers worldwide," High Power Laser Sci. Eng. **7**, e54 (2019).